Algorithms for Determining Relative Position between Spheroids and Hyperboloids with One Sheet

Paula M. Castro*, Adriana Dapena, María J. Souto-Salorio, Ana D. Tarrío-Tobar

Universidade da Coruña, A Coruña, Spain

Abstract

In this work we present a new method for determining relative positions between one moving object, modelled by a bounding spheroid, and surrounding static objects, modelled by circular hyperboloids of one sheet. The proposed strategy is based on the real-time calculation of the coefficients of degree three polynomial. We propose several algorithms for two real applications of this geometric problem: the first one, oriented to the design of video games, and the second one, devoted to surveillance tasks of a quadcopter in industrial or commercial environments.

Key words: Relative position, spheroid, hyperboloid, simulated environments, algorithms

1. Introduction

The determination of relative position and collision detection has been widely researched during the last years. These studies have been

*Corresponding author

Email addresses: paula.castro@udc.es (Paula M. Castro), adriana.dapena@udc.es (Adriana Dapena), maria.souto.salorio@udc.es (María J. Souto-Salorio), ana.dorotea.tarrio.tobar@udc.es (Ana D. Tarrío-Tobar)

mainly motivated by the extensive field of their potential applications in very-demanded recent technologies used in video games design, robotics, or physical simulations.

Collision detection and proximity query is a general problem for determining if two or more objects intersect or not, which can be solved in a geometric way [1, 2]. This geometric approach runs into problems such as the computational complexity, the storage requirements, the robustness, or the development of efficient algorithms and data structures.

Classical geometric algorithms for contact detection use quadric bounding surfaces as object modelling. For further details see [3, 4, 5, 6, 7]. The most commonly used bounding volume for contact detection is a simple approximative bounding sphere, which leads to faster tests and less memory requirements but higher false positives [8, 9]. Moreover, thus previous methods for contact detection consider only convex bodies. Recently, the authors in [10] have characterized all the possible relative positions between a circular hyperboloid of one sheet and a sphere using for this purpose the roots of a characteristic polynomial associated to these surfaces. The work [10] also provides three different tables helping to that classification according to the hyperboloid and sphere dimensions.

The first contribution of this paper is to extend the work in [10] to the detection of relative positions between spheroids and circular hyperboloids of one sheet using for this purpose the coefficients of a degree three polynomial associated to these surfaces instead of its roots, which provides a simple method for the contact detection between those two surfaces based on such an easy calculation. The second contribution of this work is the application

of this theory to very topical scenarios, as shown in [11, 12, 13], focused on detection contact between non-static and static objects. The first proposed application will be a video game environment, in which an object (a person, a robot, or an animal) moves in a scenario where one or more objects could be modelled by hyperboloids of one sheet, as for example trees. In the second proposed application, we will model *Unmanned Aerial Vehicles* (UAVs), like a quadcopter, by means of a bounding spheroid. For this application, we also propose an algorithm based on *Bounding Volume Hierarchies* (BVHs) [14, 15], which uses not only the bounding volume, but also the children ones corresponding to smaller spheroids containing the four rotors. Such a quadcopter could be used for the aforementioned applications inside a structure modelled by an hyperboloid of one sheet, like a cooling tower, a water tower, a cathedral, an air traffic control tower, and so on.

This work is organized as follows. Section 2 presents the theory of the proposed strategy for the computation of relative positions. Section 3 shows two applications: the first one, related to the design of a video game, and the second one, applied to surveillance tasks of quadcopters in hyperboloid-form structures, like cooling towers in thermal power plants or tourist buildings (see Subsections 3.1 and 3.2, respectively). Section 4 presents the BVHs strategy. Finally, some concluding remarks are made in Section 5.

2. Mathematical formulation

In this section we show how to determine the relative position between a spheroid and a circular hyperboloid of one sheet. We will use the following notation.

We consider $\overline{\mathcal{H}}$ as a circular hyperboloid of one sheet centred at the origin and described by the following equation

$$\overline{\mathcal{H}}: \quad \frac{x^2}{\alpha^2} + \frac{y^2}{\alpha^2} - \frac{z^2}{\gamma^2} = 1, \quad \text{for } \alpha, \gamma > 0. \tag{1}$$

In matrix notation, it can be expressed as follows

$$X^{\mathrm{T}} \overline{H} X - 1 = 0, \tag{2}$$

with $X = (x, y, z)^{\mathrm{T}}$ and the associated matrix

$$\overline{H} = diag\left(\frac{1}{\alpha^2}, \frac{1}{\alpha^2}, -\frac{1}{\gamma^2}\right). \tag{3}$$

Note that $^{\mathrm{T}}$ denotes the transpose operator.

We also define a spheroid $\mathcal{E}$ centred at the point $C_0 = (x_0, y_0, z_0)$ with parameters b and d, defined by the equation

$$\mathcal{E}: \quad \frac{(x-x_0)^2}{b^2} + \frac{(y-y_0)^2}{b^2} + \frac{(z-z_0)^2}{d^2} = 1, \quad \text{for } b, d > 0. \tag{4}$$

We can rewrite this expression using a matrix formulation as given

$$X^{\mathrm{T}} E X - 2BX + K = 0, \tag{5}$$

with E expressed as

$$E = diag\left(\frac{1}{b^2}, \frac{1}{b^2}, \frac{1}{d^2}\right), \tag{6}$$

and where $B = \left(\frac{x_0}{b^2}, \frac{y_0}{b^2}, \frac{z_0}{d^2}\right)$ and $K = \frac{x_0^2}{b^2} + \frac{y_0^2}{b^2} + \frac{z_0^2}{d^2} - 1$, for $b, d > 0$.

We are interested in the determination of relative position between a hyperboloid $\overline{\mathcal{H}}$ and a spheroid $\mathcal{E}$. For this purpose, we have to find the transformations that allow us to solve this problem through both the equivalent hyperboloid $\mathcal{H}$ and the sphere $\mathcal{S}$.

Theorem 1. *Contact detection between $\overline{\mathcal{H}}$ and $\mathcal{E}$ is equivalent to contact detection between $\mathcal{H}$ and $\mathcal{S}$, respectively given by*

$$\mathcal{H}: \quad \frac{x^2}{(\frac{\alpha}{b})^2} + \frac{y^2}{(\frac{\alpha}{b})^2} - \frac{z^2}{(\frac{\gamma}{d})^2} = 1, \tag{7}$$

$$\mathcal{S}: \quad \left(x - \frac{x_0}{b}\right)^2 + \left(y - \frac{y_0}{b}\right)^2 + \left(z - \frac{z_0}{d}\right)^2 = 1. \tag{8}$$

Proof:. Let consider the linear application $F : \mathbb{R}^3 \to \mathbb{R}^3$ given by $F(X) = AX$, where the matrix A is given by

$$A = diag\left(\frac{1}{b}, \frac{1}{b}, \frac{1}{d}\right). \tag{9}$$

Denoting $\overline{X} = AX$, and taking into account that A is a regular matrix and $A = A^{\mathrm{T}}$, from (2) we obtain that $\overline{X}^T H \overline{X} - 1 = 0$, which corresponds to the hyperboloid defined in (7), with

$$H = A^{-1}\overline{H}A^{-1} = diag\left(\frac{b^2}{\alpha^2}, \frac{b^2}{\alpha^2}, -\frac{d^2}{\gamma^2}\right). \tag{10}$$

Moreover, from (5) and considering that $A^{-1}EA^{-1} = I$, where I is the identity matrix, and according to (6) and (9), we have $\overline{X}^T\overline{X} - 2BA^{-1}\overline{X} + K = 0$, which corresponds to (8).

As conclusion it can be said that, since F is an isomorphism, if X is an intersection point between $\mathcal{E}$ and $\overline{\mathcal{H}}$, then $\overline{X} = F(X) = AX$ is an intersection point between $\mathcal{S}$ and $\mathcal{H}$, and vice versa. □

Considering the isomorphism given in Theorem 1, we introduce the following notation.

The characteristic polynomial for $\mathcal{S}$ and $\mathcal{H}$, respectively defined by (7) and (8), is given by

$$f(\lambda) = \frac{(a^2 + \lambda)g(\lambda)}{a^2c^2}, \tag{11}$$

with

$$g(\lambda) = \lambda^3 + (a^2 - c^2 + 1 - x_c^2 - y_c^2)\lambda^2 \\ - (a^2c^2 - a^2 + c^2 - c^2x_c^2 - c^2y_c^2 + a^2z_c^2)\lambda - a^2c^2, \tag{12}$$

where $a = (\frac{\alpha}{b})$ and $c = (\frac{\gamma}{d})$ are the parameters of the hyperboloid defined by (7), and $x_c = \frac{x_0}{b}$, $y_c = \frac{y_0}{b}$, and $z_c = \frac{z_0}{d}$ are the coordinates of the centre point of the sphere defined by (8). Notice that $\lambda = -a^2 = -\left(\frac{\alpha}{b}\right)^2$ is one root of f and that the other roots are also roots of g.

We focus our attention on finding conditions which allow us to determine if the spheroid is either exterior or interior to the hyperboloid by studying the discriminant and coefficients of g in (12).

Remark 2. *In general, for a monic degree three polynomial in the form* $x^3 + c_2x^2 + c_1x + c_0$*, the discriminant* Δ *is*

$$\Delta = -4c_2^3c_0 + c_2^2c_1^2 + 18c_2c_1c_0 - 4c_1^3 - 27c_0^2. \tag{13}$$

In our case, the coefficients c_0*,* c_1*, and* c_2 *of* g *are obtained as*

$$\begin{aligned} c_0 &= -\left(\frac{\alpha}{b}\right)^2\left(\frac{\gamma}{d}\right)^2, \\ c_1 &= -\left(\frac{\alpha}{b}\right)^2\left(\frac{\gamma}{d}\right)^2 + \left(\frac{\alpha}{b}\right)^2 - \left(\frac{\gamma}{d}\right)^2 \\ &+ \left(\frac{\gamma}{d}\right)^2\left(\frac{x_0}{b}\right)^2 + \left(\frac{\gamma}{d}\right)^2\left(\frac{y_0}{b}\right)^2 - \left(\frac{\alpha}{b}\right)^2\left(\frac{z_0}{d}\right)^2, \\ c_2 &= \left(\frac{\alpha}{b}\right)^2 - \left(\frac{\gamma}{d}\right)^2 + 1 - \left(\frac{x_0}{b}\right)^2 - \left(\frac{y_0}{b}\right)^2 - \left(\frac{z_0}{d}\right)^2. \end{aligned} \tag{14}$$

In practice, the most commonly used hyperboloid corresponds to the restriction given by $(\frac{\alpha}{b}) \geq 1$ or/and $(\frac{\gamma}{d})^2 \geq (\frac{\alpha}{b})$. Some examples of this type are the circular hyperboloids used in architecture (as cooling towers,

air traffic control towers, etc.) which are large in comparison with other surrounding objects that can collide with them (cleaning robots, UAVs, etc.) and be enclosed by a spheroid. For this reason, we will restrict our study to these cases.

In [10], the authors have studied the roots of the characteristic polynomial f for contact detection between $\mathcal{S}$ and $\mathcal{H}$. Following this work, we can obtain a characterization to determine if the spheroid $\mathcal{E}$ is exterior to the hyperboloid $\overline{\mathcal{H}}$ using for that purpose the coefficients of g.

Proposition 3. *Let $\overline{\mathcal{H}}$ and $\mathcal{E}$ verifying $(\frac{\gamma}{d})^2 \geq (\frac{\alpha}{b})$. Then:*

1. *The spheroid is exterior to the hyperboloid if and only $\Delta > 0$, $c_2 < 0$, and $c_1 > 0$.*
2. *If $\Delta \leq 0$, then there is contact between spheroid and hyperboloid.*

Proof:. By Theorem 1, the spheroid $\mathcal{E}$ is exterior to the hyperboloid $\overline{\mathcal{H}}$ if and only if the transformed sphere $\mathcal{S}$ is exterior to the transformed hyperboloid $\mathcal{H}$. If $(\frac{\alpha}{b}) \geq 1$ then the relative positions between $\mathcal{S}$ and $\mathcal{H}$ are given by Table 1 of Theorem 6 in [10]. Otherwise, the relative positions between $\mathcal{S}$ and $\mathcal{H}$ are shown in Tables 1 and 2 of Theorems 6 and 14, respectively, in [10].

From these theorems, we have that the spheroid is exterior to the hyperboloid if and only if the characteristic polynomial f has three different positive roots. Then, using (11), we have that the spheroid is exterior to the hyperboloid if and only if g has three different positive roots. By Descartes' rule of signs we know that the number of negative roots of g is the same as the number of changes in sign of the coefficients of the terms of $g(-\lambda)$ or less than this by an even number. In our case, $g(-\lambda) = (-1)\lambda^3 + c_2\lambda^2 - c_1\lambda + c_0$.

Remember that, from (14), we have that $c_0 < 0$. Therefore, it must be satisfied that $c_2 < 0$ and $c_1 > 0$ to guarantee non–negative roots for g. Then we have $c_2 < 0$ and $c_1 > 0$ if and only if all the real roots of g are positive. Now, by definition of discriminant, we have that $\Delta > 0$ (see (13)) if and only if g has three different real roots. Then we conclude that $\Delta > 0$ and $c_2 < 0$ and $c_1 > 0$ is equivalent to the fact that the spheroid is exterior to the hyperboloid. Finally, using again Theorem 6 and Theorem 14 in [10], we have that if $\Delta \leq 0$, then there is contact between spheroid and hyperboloid. □

Remark 4. *Notice that under the conditions of the previous result, i.e. for $\overline{\mathcal{H}}$ and $\mathcal{E}$ verifying $(\frac{\gamma}{d})^2 \geq (\frac{\alpha}{b})$, the discriminant and coefficients do not provide equivalent conditions for the interior case because if we analyse the cases shown in Tables 1 and 2 respectively corresponding to Theorems 6 and 14 included in [10], we extract the following conclusion: if g has two different negative roots then either there is contact or the spheroid is interior to the hyperboloid.*

The following result is obtained in a similar way using Theorems 6 and 15 of [10].

Proposition 5. *Let $\overline{\mathcal{H}}$ and $\mathcal{E}$ verifying $(\frac{\alpha}{b}) > 1$. Then:*

1. *The spheroid is interior to the hyperboloid if and only if $\Delta > 0$ and either $[c_2 > 0, c_1 \neq 0]$ or $[c_2 < 0, c_1 < 0]$.*
2. *If $\Delta \leq 0$, then there is contact between spheroid and hyperboloid.*

Remark 6. *Notice that under the conditions of the previous result, i.e. for $\overline{\mathcal{H}}$ and $\mathcal{E}$ verifying $(\frac{\alpha}{b}) \geq 1$, the discriminant and the coefficients do not*

provide equivalent conditions for the exterior case because if we analyse the cases shown in Tables 1 and 3 corresponding to Theorems 6 and 15 of [10], we can conclude that if g has three different positive roots, then either there is contact or the spheroid is exterior to the hyperboloid.

3. Real Applications of the Proposed Strategy

Simulated environments (including video games, virtual reality, etc.) are real or imaginary situations that enable user to perform operations and show their effects in real time. In this section we will show two applications to real situations in which it is needed to determine the relative position between a moving object, modelled using spheroids, and a fixed object, modelled using a hyperboloid. Before doing any movement, the updated position is pre–determined so that our proposed algorithm indicates if it is valid or non-valid movement.

3.1. Application 1: Video Game Environment

In order to show how to use our results in this type of applications, Fig. 1 shows a moving object (a woman) and the surrounding static ones (trees). The woman is modelled with a simple spheroid although more accurate approximations using a higher number of spheroids to individually model legs, arms, etc., can be easily extended. This object can do any displacement in the x–axis, y–axis, and z–axis without exceeding the z–dimension of the static object, or rotations in the xy–plane. The tree trunks are modelled by hyperboloids satisfying the $(\frac{\gamma}{d})^2 \geq (\frac{\alpha}{b})$ condition. Thus, as you can see in the figure, the hyperboloid marked as "type 1" corresponds to the $(\frac{\alpha}{b}) \geq 1$ condition, i.e., the tree trunk is wider than the woman; otherwise,

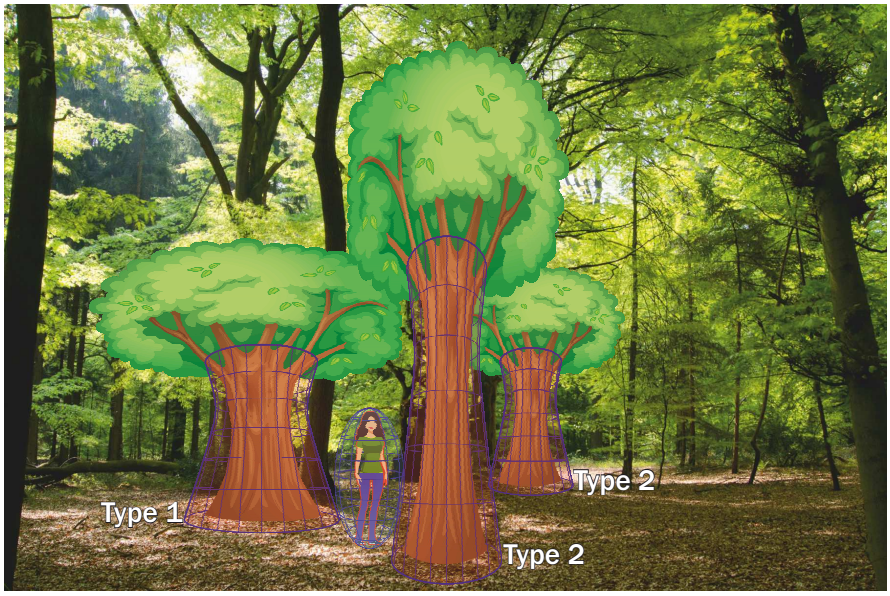

Figure 1: Application 1. A woman moving in a simulated forest environment.

the hyperboloids marked as "type 2" correspond to the $(\frac{\alpha}{b}) < 1$ case. From the first condition of Proposition 3, we propose the Procedure 1 (Table 1) to detect valid movements (i.e, those for which the woman bounding spheroid is "exterior" to the trunk bounding hyperboloid).

compute c_0, c_1, c_2 using (14) and Δ using (13);

if $\Delta > 0$ *and* $c_2 < 0$ *and* $c_1 > 0$ **then**
| "valid movement";

else
| "non–valid movement";

end

Table 1: P

rocedure 1 for video game, with $(\frac{\gamma}{d})^2 \geq (\frac{\alpha}{b})$ and $\mathcal{E}$ exterior to $\overline{\mathcal{H}}$. This procedure is valid for both cases $(\frac{\alpha}{b}) \geq 1$ and $(\frac{\alpha}{b}) < 1$.

Data: values of α, γ, b, and d;

Result: $valid = 1$ for valid movement (exterior position) or $valid = 0$ for non-valid movement (interior position or contact);

$A \leftarrow (\alpha/b)^2$

$B \leftarrow (\gamma/d)^2$

$c_0 \leftarrow -A \times B$

$C \leftarrow c_0 + A - B$

while *movement* **do**

$(x_0, y_0, z_0) \leftarrow obtain\_position$

$P \leftarrow (x_0^2 + y_0^2)/b^2$

$Q \leftarrow (z_0/d)^2$

$c_1 \leftarrow C + B \times P - A \times Q$

$c_2 \leftarrow A - B + 1 - P - Q$

$\Delta \leftarrow -4 \times c_2^3 \times c_0 + (c_2 \times c_1)^2 + 18 \times c_2 \times c_1 \times c_0 - 4 \times c_1^3 - 27 \times c_0^2$

$valid \leftarrow (\Delta > 0)$ and $(c_2 < 0)$ and $(c_1 > 0)$;

end

Table 2: Pseudocode of Procedure 1 for video game.

From (14) and (13), we can write the pseudocode of Procedure 1 (Table 1) as given in Table 2, where the number of operations has been optimized considering that some terms are computed independently from sphere location. Since only additions or products are performed, the computational cost is very low (see [16]).

This procedure exhibits several advantages compared to previous approaches. Our proposal in [13] determines relative positions considering the roots of the polynomial f given in (12), instead of computing only the coefficients, which implies to evaluate trigonometric functions when $\Delta > 0$. Moreover, other methods described in [3, 4, 5, 6, 7] can not be used for the application shown in this section since moving and static objects are modelled by quadric bounding surfaces.

3.2. Application 2: UAV Control Environment

Because of its potential for commercial, military, law-enforcement, research, and other purposes, UAVs have received considerable attention in recent years in real and simulated environment [12]. Contact detection methods based on computing the distance from the UAV to the surface are adequate in most situations where that surface shape is similar for all height positions but hyperboloid structures have not this property. Figure 2 shows two hyperboloid structures bounded by the corresponding hyperboloid volume: the left picture represents a cooling tower, and the right one, a touristic tower.

We consider that the UAV flies inside the cooling tower following a trajectory with three types of possible movements: *pitch*, forward and backward UAV tilt; *yaw*, left and right UAV rotation in the xy–plane, without changing the z–axis, and *throttle*, vertical up and down UAV motion, varying only the z–axis. Note that this last displacement must be restricted up to the maximum height of the cooling tower.

Figure 3 shows the geometric model of an example of UAV, a quadcopter. Observe that this quadcopter can be bounded by an exterior spheroid with

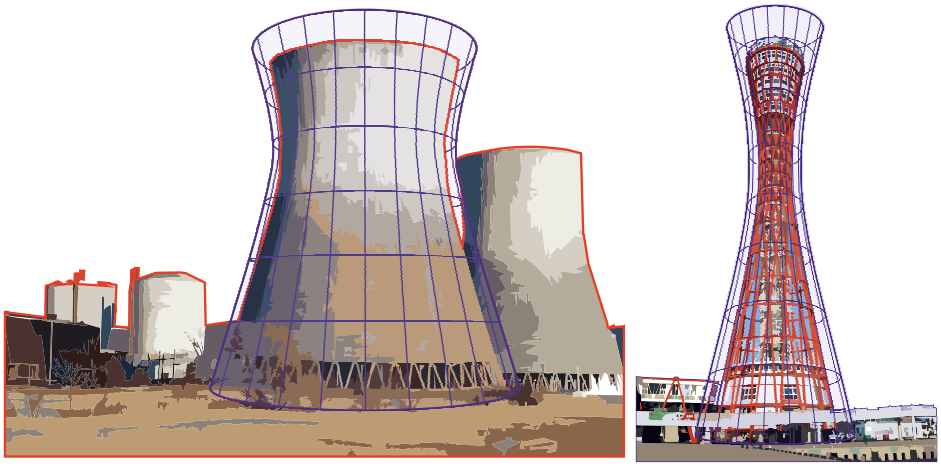

(a) Meirama Cooling Tower (Spain) (b) Kobe Tower (Japan)

Figure 2: Application 2. One-sheeted hyperboloid structures.

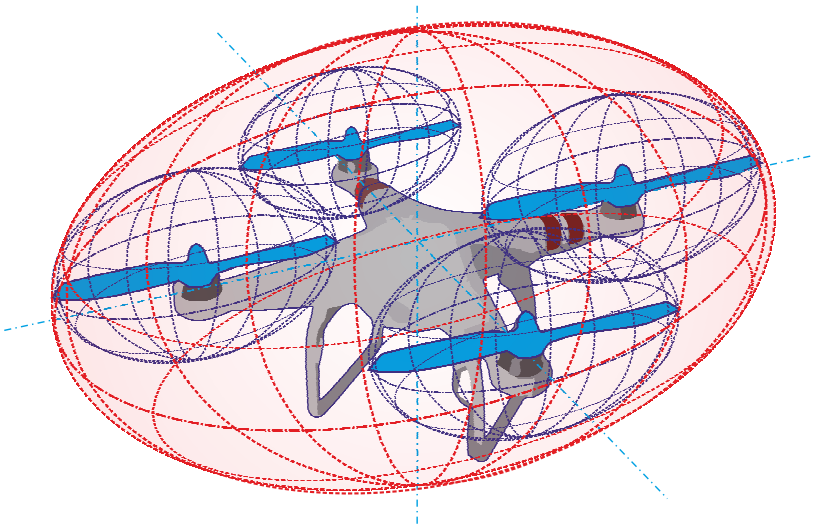

Figure 3: Application 2. Model of a quadcopter with a bounding spheroid and four smaller spheroids bounding each rotor.

centre (x_0, y_0, z_0) and parameters b and d. The i–th rotor, $i = 1, 2, 3, 4$, is bounded by its corresponding smaller spheroid, denoted by $\mathcal{E}_i$, with centre point (x_i, y_i, z_i) and parameters b_s and d_s, identical for all spheroids. The Cartesian coordinates of the centre point is given by the following expressions

$$\begin{aligned} x_i &= x_0 + \frac{l\sqrt{2}}{2}(\cos(g_i) - \sin(g_i)) = x_0 + \frac{l\sqrt{2}}{2}T_1(g_i), \\ y_i &= y_0 + \frac{l\sqrt{2}}{2}(\cos(g_i) + \sin(g_i)) = y_0 + \frac{l\sqrt{2}}{2}T_2(g_i), \\ z_i &= z_0, \end{aligned} \tag{15}$$

where $T_1(g_i)$ and $T_2(g_i)$ are obviously given by $T_1(g_i) = \cos(g_i) - \sin(g_i)$ and $T_2(g_i) = \cos(g_i) + \sin(g_i)$, respectively. Notice that, in general, the angles of the spheroids $\mathcal{E}_2$, $\mathcal{E}_3$, and $\mathcal{E}_4$ can be computed from the angle of $\mathcal{E}_1$, denoted as g_1, by using $g_i = g_1 + \frac{(i-1)\pi}{2}$, $i = 2, 3, 4$, respectively.

Contact detection between the hyperboloid $\overline{\mathcal{H}}$ and the spheroid $\mathcal{E}_i$ is equivalent to contact detection between the hyperboloid $\mathcal{H}_s$ and the sphere $\mathcal{S}_i$, where

$$\mathcal{H}_s: \quad \frac{x^2}{\left(\frac{\alpha}{b_s}\right)^2} + \frac{y^2}{\left(\frac{\alpha}{b_s}\right)^2} - \frac{z^2}{\left(\frac{\gamma}{d_s}\right)^2} = 1, \tag{16}$$

$$\mathcal{S}_i: \quad \left(x - \frac{x_i}{b_s}\right)^2 + \left(y - \frac{y_i}{b_s}\right)^2 + \left(z - \frac{z_i}{d_s}\right)^2 = 1. \tag{17}$$

Considering (15) and applying $T_1(g_i)^2 + T_2(g_i)^2 = 2$, we have that

$$\begin{aligned} x_i^2 + y_i^2 &= \left(x_0 + \frac{l\sqrt{2}}{2}T_1(g_i)\right)^2 + \left(y_0 + \frac{l\sqrt{2}}{2}T_2(g_i)\right)^2 \\ &= x_0^2 + y_0^2 + l^2 + l\sqrt{2}(T_1(g_i)x_0 + T_2(g_i)y_0). \end{aligned} \tag{18}$$

Observe that the c_0 coefficient in (14) does not depend on the centre

point. Then, for all the spheroids $\mathcal{E}_i$ it verifies

$$c_{0,s} = -\left(\frac{\alpha}{b_s}\right)^2 \left(\frac{\gamma}{d_s}\right)^2. \tag{19}$$

We introduce the following expressions,

$$\begin{aligned} C(g_i) &= \frac{l\sqrt{2}(T_1(g_i)x_0 + T_2(g_i)y_0)}{b_s^2}, \\ B_1 &= 1 - \left(\frac{\gamma}{d_s}\right)^2 - \left(\frac{z_0}{d_s}\right)^2, \\ B_2 &= \frac{x_0^2 + y_0^2 + l^2}{b_s^2}. \end{aligned} \tag{20}$$

As shown in Appendix A, we obtain the final expressions

$$\begin{aligned} c_1(g_i) &= \left(\frac{\alpha}{b_s}\right)^2 B_1 + \left(\frac{\gamma}{d_s}\right)^2 (B_2 - 1 + C(g_i)), \\ c_2(g_i) &= \left(\frac{\alpha}{b_s}\right)^2 + B_1 - B_2 - C(g_i). \end{aligned} \tag{21}$$

Considering that the quadcopter flies in the interior of this hyperboloid, Procedure 2.a (Table 3) allows to detect when a movement is valid or not. We will use Proposition 5 to determine non-valid movements. This method can be applied if $(\frac{\alpha}{b_s}) \geq 1$.

compute $c_{0,s}$, $c_1(g_i)$, and $c_2(g_i)$ for $i = 1, 2, 3, 4$ using (19) and (21), and $\Delta(g_i)$ using (13);

if $\Delta(g_i) \leq 0$ *for some spheroid* $\mathcal{E}_i$, $i = 1, 2, 3, 4$, **then**
| "non–valid movement";

else
| **if** $[c_2(g_i) > 0; c_1(g_i) \neq 0]$ *or* $[c_2(g_i) < 0; c_1(g_i) < 0]$ *for all spheroid* $\mathcal{E}_i$, $i = 1, 2, 3, 4$, **then**
| | "valid movement";
| **else**
| | "non–valid movement";
| **end**

end

Table 3: Procedure 2.a for UAV control, with $(\frac{\alpha}{b_s}) \geq 1$ and $\mathcal{E}_i$ interior to $\overline{\mathcal{H}}$.

Notice that (19), (20), and (21) indicate that the coefficients $c_{0,s}$, $c_1(g_i)$, and $c_2(g_i)$ can be determined without computing the angle g_i of each spheroid. As a consequence, similar operations to those shown throughout of the pseudocode of Procedure 1 (Table 2) could be performed.

4. Bounding Volume Hierarchicy

A BVH is based on modelling an object using a tree structure of bounding volumes that form the leaf nodes of the tree which are grouped and enclosed by other larger bounding volumes in a recursive way, eventually resulting in a tree structure with a single bounding volume at the top of the tree. Sphere and spheroid tree hierarchies are simple to be implemented and suitable for efficient minimum computation (see, for instance, [14, 15] and references therein).

The procedures proposed in the previous section could be used to detect valid or non-valid movements in a hierarchy structure, when the objects and their individual components can be enclosed by spheroids. As an example, we will consider the application for UAV control described in Subsection 3.2.

We consider that the rotors are bounded by small spheroids and they are then bounded by a bigger one (see Fig. 3). Procedure 2.b (Table 4 is used to detect valid and non-valid movements. Firstly, we would analyse the big bounding spheroid $\mathcal{E}$ assuming the condition $(\frac{a}{b}) \geq 1$ in Proposition 5. If the procedure detects contact, i.e. $\Delta \leq 0$, we would consider each one of the smaller spheroids, as was directly done in Procedure 2.a (Table 3) to discard false collision detections. Otherwise, we consider the condition given in the same proposition to verify that the movement is interior.

compute c_0, c_1, c_2 using (14), and Δ using (13) ;

if $\Delta \leq 0$ **then**

  compute $c_{0,s}$, $c_1(g_i)$ and $c_2(g_i)$ for $i = 1, 2, 3, 4$ using (19) and (21), and $\Delta(g_i)$ using (13);

  if $\Delta(g_i) \leq 0$ *for some spheroid* $\mathcal{E}_i$, $i = 1, 2, 3, 4$, **then**

    "non–valid movement"

  else

    if $[c_2(g_i) > 0; c_1(g_i) \neq 0]$ *or* $[c_2(g_i) < 0; c_1(g_i) < 0]$ *for all spheroid* $\mathcal{E}_i$, $i = 1, 2, 3, 4$, **then**

      "valid movement"

    else

      "non–valid movement"

    end

  end

else

  if $[c_2 > 0; c_1 \neq 0]$ *or* $[c_2 < 0; c_1 < 0]$ **then**

    "valid movement"

  else

    "non–valid movement"

  end

end

Table 4: Procedure 2.b for UAV control, with $(\frac{\alpha}{b}) \geq 1$ and $\mathcal{E}$ interior to $\overline{\mathcal{H}}$. This algorithm is valid for both cases $(\frac{\gamma}{d})^2 \geq (\frac{\alpha}{b})$ and $(\frac{\gamma}{d})^2 < (\frac{\alpha}{b})$.

Notice that the pseudocode corresponding to the condition $\Delta \leq 0$ in Procedure 2.b (Table 4) is the same as that of Procedure 2.a (Table 3). Since the computation of $\Delta(g_i)$ has a considerable computational cost in

comparison to other operations, we are interested in counting when $\Delta \leq 0$. Towards this end, we consider a computer simulated environment where the hyperboloid models the cooling tower of a power station. This tower has $\alpha = 2$ m and $\gamma = 35.6/2$ m. The UAV is bounded by a spheroid with $b = 0.25$ m and $d = 0.15$ m and the rotors are wrapped in spheroids with $b_s = 0.1$ m and $d_s = 0.05$ m.

The UAV flies inside the cooling tower following a random trajectory determined as follows:

- straight movement with probability 0.25,
- down or up movement with probability 0.25,
- random turn with angle in $[-\pi/4, \pi/4]$ with probability 0.5,
- and turn of angle $-\pi/2$ or $\pi/2$ if a non-valid movement is detected with Procedure 2.a (Table 3).

For instance, Fig. 4 shows the 3D and the 2D views, respectively in subfigures (a) and (b), of three trajectories of 25 positions. Figure 4 (c) shows the values of the discriminant Δ obtained using (13). The values of Δ closest to zero correspond to those situations where the UAV is near the tower walls.

We consider now that the UAV follows a trajectory of $D = 500$ m with a speed v varying from 5 m/s to 10 m/s. Before any movement, the UAV evaluates Procedure 2.b (Table 4) to determine if the movement is valid. This prediction is done considering the position of the UAV in t seconds, i.e. its response time. For a non-valid movement, the UAV turns and tries a new one.

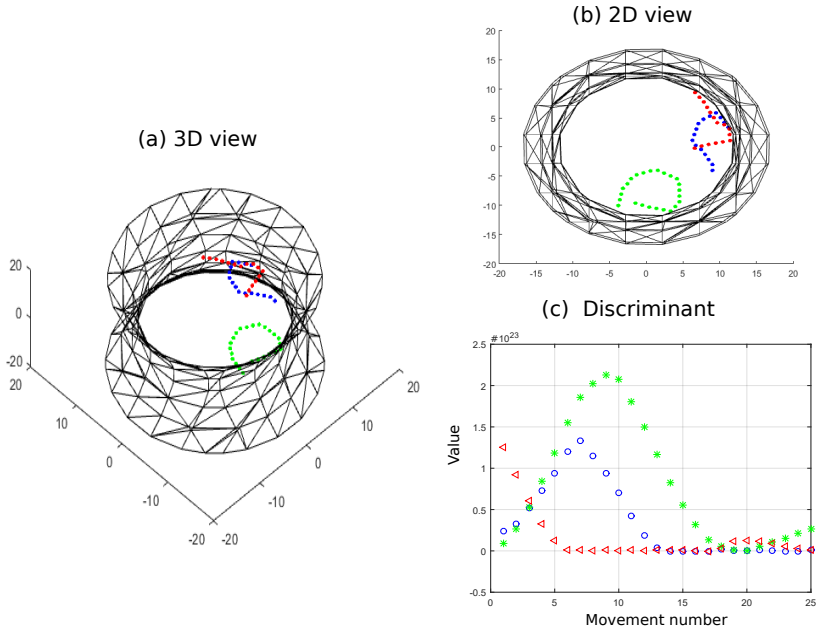

Figure 4: Application 2. Trajectory and values of Δ.

Table 5 shows the number of executions in a trajectory, expressed as a percentage and averaged from 1 000 realizations, where $\Delta \leq 0$ in Procedure 2.b (Table 4). We will referred to as execution percentage. As you can see in the table, we obtain less than 14 % of execution percentage for all cases, which represents an extremely low ratio. Note that for $t = 0.1$ m/s the values are similar independently from speed. Otherwise, this percentage is reduced as speed increases since higher speeds lead to higher probabilities of obtaining interior or exterior positions, which correspond to $\Delta > 0$. This also happens for increasing t values. Again, the probability of interior or exterior positions will be higher.

Table 5: Percentage of executions of $\Delta \leq 0$ in Procedure 2.b (Table 4)

	v (m/s)					
t (s)	5	6	7	8	9	10
0.1	13.9532	13.9029	13.5640	13.1907	12.9477	12.4708
0.2	11.7990	10.9387	10.3449	9.6364	8.9626	8.5885
0.3	10.9574	10.2549	9.4475	8.6942	7.8514	7.4627

5. Conclusions

We have focused this work on the determination of relative position between two types of bounding volumes: a spheroid, which moves in a static environment, and all those surrounding objects that can be modelled by hyperboloids of one sheet. We show how this method could be used in recent applications. Applying the developed theory, we propose three algorithms with the goal of reducing the computational complexity using more adequate bounding volumes than the standard approaches.

A. Calculation of expressions $c_1(g_i)$ and $c_2(g_i)$

In this appendix we obtain the expressions of $c_1(g_i)$ and $c_2(g_i)$ in Application 2 corresponding to the UAV movement inside a cooling tower. Substituting (15) into c_1 given by (14), we have

$$c_1(g_i) = \left(\frac{\alpha}{b_s}\right)^2 \left(1 - \left(\frac{\gamma}{d_s}\right)^2 - \left(\frac{z_i}{d_s}\right)^2\right) + \left(\frac{\gamma}{d_s}\right)^2 \left(\frac{x_i^2 + y_i^2}{b_s^2} - 1\right).$$

Using (18), we can express $c_1(g_i)$ as follows

$$\begin{aligned}
c_1(g_i) &= \left(\frac{\alpha}{b_s}\right)^2 \left(1 - \left(\frac{\gamma}{d_s}\right)^2 - \left(\frac{z_0}{d_s}\right)^2\right) \\
&\quad + \left(\frac{\gamma}{d_s}\right)^2 \left(\frac{x_0^2 + y_0^2 + l^2 + l\sqrt{2}(T_1(g_i)x_0 + T_2(g_i)y_0)}{b_s^2} - 1\right) \\
&= \left(\frac{\alpha}{b_s}\right)^2 \left(1 - \left(\frac{\gamma}{d_s}\right)^2 - \left(\frac{z_0}{d_s}\right)^2\right) \\
&\quad + \left(\frac{\gamma}{d_s}\right)^2 \left(\frac{x_0^2 + y_0^2 + l^2 + l}{b_s^2} - 1\right) + \left(\frac{\gamma}{d_s}\right)^2 \left(\frac{l\sqrt{2}(T_1(g_i)x_0 + T_2(g_i)y_0)}{b_s^2}\right).
\end{aligned}$$

If we define

$$\begin{aligned}
C(g_i) &= \frac{l\sqrt{2}(T_1(g_i)x_0 + T_2(g_i)y_0)}{b_s^2}, \\
A_1 &= \left(\frac{\alpha}{b_s}\right)^2 \left(1 - \left(\frac{\gamma}{d_s}\right)^2 - \left(\frac{z_0}{d_s}\right)^2\right) + \left(\frac{\gamma}{d_s}\right)^2 \left(\frac{x_0^2 + y_0^2 + l^2}{b_s^2} - 1\right),
\end{aligned}$$

$c_1(g_i)$ could be consequently rewritten in this way

$$c_1(g_i) = A_1 + \left(\frac{\gamma}{d_s}\right)^2 C(g_i).$$

Using a similar reasoning, $c_2(g_i)$ can be expressed as

$$c_2(g_i) = A_2 - C(g_i),$$

where

$$A_2 = \left(\frac{\alpha}{b_s}\right)^2 + 1 - \left(\frac{\gamma}{d_s}\right)^2 - \left(\frac{z_0}{d_s}\right)^2 - \frac{x_0^2 + y_0^2 + l^2}{b_s^2}.$$

Now, defining

$$\begin{aligned}
B_1 &= 1 - \left(\frac{\gamma}{d_s}\right)^2 - \left(\frac{z_0}{d_s}\right)^2, \\
B_2 &= \frac{x_0^2 + y_0^2 + l^2}{b_s^2},
\end{aligned} \tag{22}$$

we obtain the expressions

$$c_1(g_i) = \left(\frac{\alpha}{b_s}\right)^2 B_1 + \left(\frac{\gamma}{d_s}\right)^2 (B_2 - 1 + C(g_i)),$$
$$c_2(g_i) = \left(\frac{\alpha}{b_s}\right)^2 + B_1 - B_2 - C(g_i). \tag{23}$$

Acknowledgment

This work has been funded by the Xunta de Galicia (ED431C 2016-045, ED341D R2016/012, ED431G/01), the Agencia Estatal de Investigación of Spain (TEC2013-47141-C4-1-R, TEC2015-69648-REDC, TEC2016-75067-C4-1-R) and ERDF funds of the EU (AEI/FEDER, UE).

The authors wish to thank José Sanmartín for his helpful work in the graphic design of the pictures included in this paper.

References

[1] P. Jiménez, F. Thomas, C. Torras, 3d collision detection: a survey, Computers & Graphics 25 (2) (2001) 269–285.

[2] R. Weller, A brief overview of collision detection, in: New Geometric Data Structures for Collision Detection and Haptics, Springer, 2013, pp. 9–46.

[3] Y.-K. Choi, J.-W. Chang, W. Wang, M.-S. Kim, G. Elber, Continuous collision detection for ellipsoids, IEEE Transactions on visualization and Computer Graphics 15 (2) (2009) 311–325.

[4] X. Jia, Y.-K. Choi, B. Mourrain, W. Wang, An algebraic approach to continuous collision detection for ellipsoids, Computer Aided Geometric Design 28 (3) (2011) 164–176.

[5] X. Jia, W. Wang, Y.-K. Choi, B. Mourrain, C. Tu, Continuous detection of the variations of the intersection curve of two moving quadrics in 3-dimensional projective space, Journal of Symbolic Computation 73 (2016) 221–243.

[6] J. Z. Levin, Mathematical models for determining the intersections of quadric surfaces, Computer Graphics and Image Processing 11 (1) (1979) 73–87.

[7] W. Wang, Y.-K. Choi, B. Chan, M.-S. Kim, J. Wang, Efficient collision detection for moving ellipsoids using separating planes, Computing 72 (1) (2004) 235–246.

[8] P. M. Hubbard, Approximating polyhedra with spheres for time-critical collision detection, ACM Transactions on Graphics (TOG) 15 (3) (1996) 179–210.

[9] K. Fischer, B. Gärtner, The smallest enclosing ball of balls: combinatorial structure and algorithms, International Journal of Computational Geometry & Applications 14 (04n05) (2004) 341–378.

[10] M. Brozos-Vázquez, M. J. Pereira-Sáez, M. J. Souto-Salorio, A. D. Tarrío-Tobar, Clasification of the relative positions between a circular hyperboloid of one sheet and a sphere, Mathematical Methods in the Applied Sciences 41 (13) (2018) 5274–5292.

[11] T. Uchiki, T. Ohashi, M. Tokoro, Collision detection in motion simulation, Computers & Graphics 7 (3-4) (1983) 285–293.

[12] G. Fasano, D. Accardo, A. Moccia, C. Carbone, U. Ciniglio, F. Corraro, S. Luongo, Multi-sensor-based fully autonomous non-cooperative collision avoidance system for unmanned air vehicles, Journal of Aerospace Computing, Information, and Communication 5 (10) (2008) 338–360.

[13] A. Dapena, M. J. Souto-Salorio, A. D. Tarrío-Tobar, P. M. Castro, An algebraic collision avoidance approach for unmanned aerial vehicle, in: 14th International Conference on Informatics in Control, Automation and Robotics (ICINCO), 2017.

[14] D. L. James, D. K. Pai, BD-tree: output-sensitive collision detection for reduced deformable models, ACM Transactions on Graphics (TOG) 23 (3) (2004) 393–398.

[15] K. Steinbach, J. Kuffner, T. Asfour, R. Dillmann, Efficient collision and self-collision detection for humanoids based on sphere trees hierarchies, in: Humanoid Robots, 2006 6th IEEE-RAS International Conference on, IEEE, 2006, pp. 560–566.

[16] G. H. Golub, C. F. Van Loan, Matrix Computations, 3rd Edition, The Johns Hopkins University Press, 1996.